LETTERS

Macrophage-specific PPARγ controls alternative activation and improves insulin resistance

Justin I. Odegaard[1,2]*, Roberto R. Ricardo-Gonzalez[1,2]*, Matthew H. Goforth[1], Christine R. Morel[1], Vidya Subramanian[4], Lata Mukundan[1], Alex Red Eagle[1,3], Divya Vats[1], Frank Brombacher[5], Anthony W. Ferrante[4] & Ajay Chawla[1,2]

Obesity and insulin resistance, the cardinal features of metabolic syndrome, are closely associated with a state of low-grade inflammation[1,2]. In adipose tissue chronic overnutrition leads to macrophage infiltration, resulting in local inflammation that potentiates insulin resistance[3,4]. For instance, transgenic expression of *Mcp1* (also known as chemokine ligand 2, Ccl2) in adipose tissue increases macrophage infiltration, inflammation and insulin resistance[5,6]. Conversely, disruption of *Mcp1* or its receptor *Ccr2* impairs migration of macrophages into adipose tissue, thereby lowering adipose tissue inflammation and improving insulin sensitivity[5,7]. These findings together suggest a correlation between macrophage content in adipose tissue and insulin resistance. However, resident macrophages in tissues display tremendous heterogeneity in their activities and functions, primarily reflecting their local metabolic and immune microenvironment[8]. While *Mcp1* directs recruitment of pro-inflammatory classically activated macrophages to sites of tissue damage[5,8], resident macrophages, such as those present in the adipose tissue of lean mice, display the alternatively activated phenotype[9]. Despite their higher capacity to repair tissue[10], the precise role of alternatively activated macrophages in obesity-induced insulin resistance remains unknown. Using mice with macrophage-specific deletion of the peroxisome proliferator activated receptor-γ (PPARγ), we show here that PPARγ is required for maturation of alternatively activated macrophages. Disruption of PPARγ in myeloid cells impairs alternative macrophage activation, and predisposes these animals to development of diet-induced obesity, insulin resistance, and glucose intolerance. Furthermore, gene expression profiling revealed that downregulation of oxidative phosphorylation gene expression in skeletal muscle and liver leads to decreased insulin sensitivity in these tissues. Together, our findings suggest that resident alternatively activated macrophages have a beneficial role in regulating nutrient homeostasis and suggest that macrophage polarization towards the alternative state might be a useful strategy for treating type 2 diabetes.

To distinguish between the pathogenic and reparative functions of macrophages in metabolic disease, we sought to identify transcriptional regulators that control alternative macrophage activation. Notably, PPARγ, a genetic sensor of fatty acids[11], is markedly induced in macrophages stimulated with interleukin-4 (IL-4)[12,13], prompting us to examine its role in alternative macrophage activation. Because Balb/c mice—but not C57Bl/6 mice—can fully support maturation of alternatively activated macrophages[14], we generated macrophage-specific PPARγ knockout (Mac-PPARγ KO) mice on the T helper 2 (Th2)-permissive Balb/c strain (see Methods). Quantitative polymerase chain reaction (Q-PCR) analysis of genomic DNA from peritoneal elicited cells and bone-marrow-derived macrophages showed high excision efficiency (~85–90%) in Mac-PPARγ KO animals (Supplementary Fig. 1a). Immunoblot analysis further confirmed the absence of PPARγ protein in bone-marrow-derived macrophages from Mac-PPARγ KO mice (Supplementary Fig. 1b). Verifying a critical role for PPARγ in alternative activation, arginase I messenger RNA and activity—both hallmarks of alternatively activated macrophages[10]—were reduced by 40% and 50%, respectively, in IL-4 stimulated PPARγ null bone-marrow-derived macrophages (Supplementary Fig. 1c and Fig. 1a).

To determine whether the arginase I gene is a direct transcriptional target of PPAR/RXR heterodimers, we analysed its promoter region for PPAR response elements. A putative PPAR response element was identified in the distal enhancer of the arginase I gene, a region known to be essential for its expression in alternatively activated macrophages[15]. Electromobility gel shift assays confirmed that PPAR/RXR heterodimers bound to the identified site in a sequence-specific manner (Supplementary Fig. 1d). To verify that PPARγ/RXR heterodimers can activate the arginase I promoter *in vivo*, cells of the mouse macrophage cell line RAW264.7 were transiently transfected with luciferase reporter construct driven by ~4 kilobases (kb) of mouse arginase I promoter/enhancer. Treatment of transfected macrophages with IL-4 led to a ~9-fold increase in luciferase activity (Fig. 1b). Moreover, the addition of PPARγ and its ligand, rosiglitazone, enhanced the ability of IL-4 to activate the arginase I promoter (twice the IL-4 stimulated level), demonstrating that PPARγ directly regulates this important facet of macrophage activation. Because alternatively activated macrophages can counteract excessive secretion of pro-inflammatory cytokines[13], we examined whether IL-4 could appropriately attenuate lipopolysaccharide-induced TNFα and IL-6 secretion. Although lipopolysaccharide-stimulated release of TNFα and IL-6 was not significantly different between the two genotypes (Fig. 1c and Supplementary Fig. 1e), IL-4 failed to suppress the secretion of IL-6 in macrophages deficient in PPARγ (Fig. 1c), which indicates that a subset of IL-4 dependent anti-inflammatory responses are regulated by PPARγ.

We recently reported that a switch to oxidative metabolism is an integral component of alternative macrophage activation[13]. Because PPARs regulate fatty acid homeostasis in many cell types[16], we investigated the requirement for PPARγ or PPARδ (the two major PPAR subtypes expressed in murine macrophages) in controlling this oxidative switch. Surprisingly, PPARγ, rather than PPARδ, was required for IL-4 induced increase in β-oxidation of fatty acids, as shown by the

[1]Division of Endocrinology, Metabolism and Gerontology, Department of Medicine. [2]Graduate Program in Immunology, [3]Department of Genetics, Stanford University School of Medicine, Stanford, California 94305-5103, USA. [4]Department of Medicine, Naomi Berrie Diabetes Center, Columbia University College of Physicians and Surgeons, New York, New York 10032, USA. [5]Institute of Infectious Disease and Molecular Medicine, Division of Immunology, Health Science Faculty, University of Cape Town, Werhner Beit South, Observatory, 7925, Anzioroad, Cape Town, South Africa.
*These authors contributed equally to this work.

~70% reduction in the rate of fatty acid oxidation in IL-4-stimulated PPARγ null macrophages (Fig. 1d). In agreement with this genetic data, ligand activation of PPARγ led to a doubling of the rate of β-oxidation (Supplementary Fig. 1f). Moreover, Q-PCR analyses with reverse transcription revealed that expression of genes controlling lipolysis (*Lpl*), fatty acid uptake (*CD36*), and oxidation (*Acadm*, *Acadl*) was reduced in IL-4-stimulated PPARγ null macrophages (Supplementary Fig. 1g). In contrast, fatty acid uptake rates were similar in control and Mac-PPARγ KO macrophages (Supplementary Fig. 1h).

An increase in cellular mitochondrial content accompanies this metabolic switch, so we tested the requirement for PPARγ in mitochondrial biogenesis. Cellular staining with MitoTracker Green revealed an absolute requirement for PPARγ in mediating the biogenic effects of IL-4 (Fig. 1e). Fluorescence microscopy with MitoTracker Red further verified that reduction in respiring mitochondria largely accounted for the observed decrease in total mitochondria in these cells (Supplementary Fig. 1i). Consistent with these findings, IL-4 failed to induce the mitochondrial proteins cytochrome C and voltage-dependent anion chanel 1 (VDAC1) in PPARγ-deficient macrophages (Fig. 1f). Lastly, the observed impairment in alternative activation was independent of the upstream IL-4 signalling pathway, because PPARγ-deficient macrophages expressed similar levels of IL-4Rα protein on their cell surface and stimulation with IL-4 resulted in equivalent levels of phosphorylation of the transcription factor STAT6 (Supplementary Fig. 2a, b).

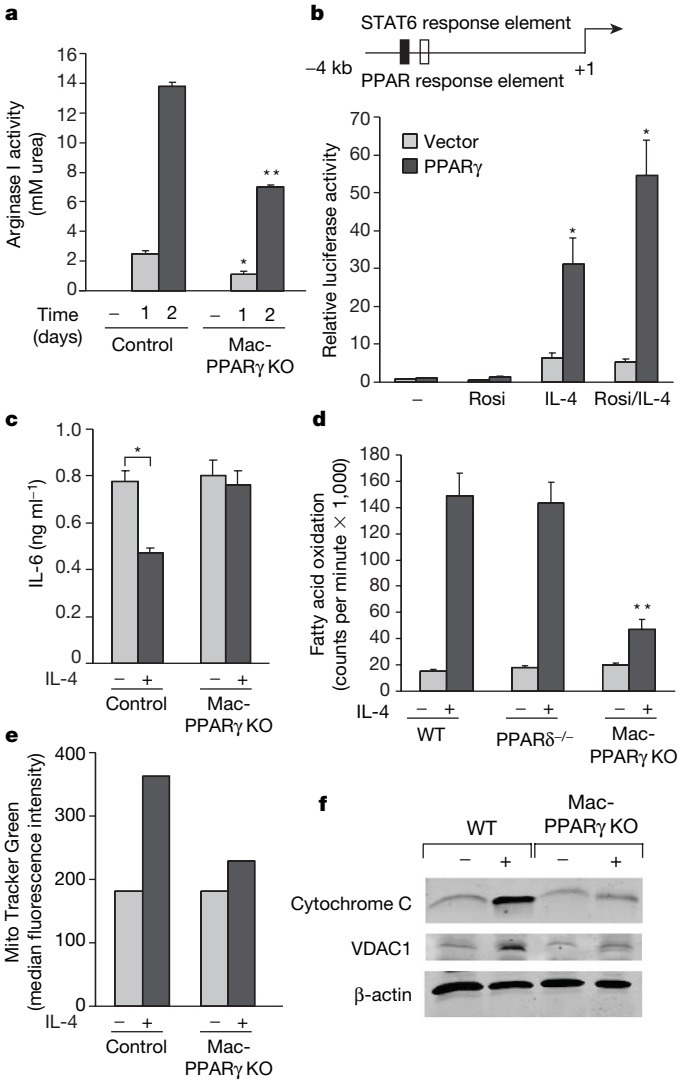

Figure 1 | PPARγ regulates alternative macrophage activation. **a**, Decreased induction of arginase I activity by IL-4 in PPARγ null macrophages. **b**, Activation of arginase I promoter by PPARγ/RXR heterodimers. Rosi, rosiglitazone. **c**, PPARγ is required for suppression of IL-6 production in alternatively activated macrophages. **d**, PPARγ is required for macrophage oxidative metabolism. Fatty acid oxidation rates were quantified in control, PPARδ null and PPARγ null bone-marrow-derived macrophages 96 h after stimulation with IL-4. **e**, **f**, IL-4 fails to induce mitochondrial biogenesis in PPARγ-deficient macrophages, as measured by Mito Tracker Green (**e**) and cytochrome C and VDAC1 (**f**) protein levels. Equivalent loading was confirmed by immunoblotting for β-actin. Data presented as mean ± s.e.m. $^{*}P < 0.05$; $^{**}P < 0.01$.

To provide an independent test for whether PPARγ can regulate the macrophage program of alternative activation *in vivo*, we used an immunological model for studying macrophage Th2-type responses. Cutaneous infection with *Leishmania major* in Th2-biased Balb/c mice leads to non-healing lesions, whereas the Th1-prone C57Bl/6 mice are resistant to acute infection[17]. Importantly, because impairment in alternative macrophage activation can delay disease progression in Balb/c mice[18], we investigated whether Mac-PPARγ KO mice were also resistant to cutaneous leishmaniasis. Indeed, Mac-PPARγ KO mice had significantly less footpad swelling 5–7 weeks after injection of *L. major* promastigotes (Fig. 2a). Lesions in Mac-PPARγ KO started to stabilize after 7 weeks, but the footpads of control mice continued to enlarge and rapidly underwent necrosis (Fig. 2b). Consistent with local extension of disease, the draining popliteal lymph nodes were hypercellular and enlarged in control mice (Supplementary Fig. 3). Because these results mimic the phenotype of mice lacking alternatively activated macrophages, our data strongly suggest that PPARγ is required for acquisition and maintenance of the alternatively activated phenotype.

On the basis of these results, we tested whether genetic deletion of PPARγ in macrophages would exacerbate the development of metabolic syndrome. Cohorts of control and Mac-PPARγ KO mice were challenged with a high fat diet for 18 weeks to promote maximal infiltration of macrophages into adipose tissue[4]. Surprisingly, Mac-PPARγ KO mice gained more weight than control mice on the high fat diet. After 17 weeks on a high fat diet, the body weight of Mac-PPARγ KO mice (46.7 ± 2.3 g) exceeded that of control mice (40.3 ± 1.2 g) by ~15% (Fig. 3a). Dual-energy X-ray absorptiometry showed a 20% increase in total fat mass and a 12% increase in adiposity in Mac-PPARγ KO animals (Fig. 3b). Consistent with an increase in adiposity, epididymal fat pads were larger (~18% by mass) and serum leptin levels were higher (~57%) in Mac-PPARγ KO mice (Supplementary Fig. 4a, b)[19]. However, adipocyte cell size was not significantly different (Supplementary Fig. 4c, d).

To define the alterations in adipose tissue better, we quantified the transcript levels of genes important in adipocyte differentiation and fatty acid metabolism. As shown in Fig. 3c, mRNA levels of a large number of genes involved in nutrient uptake, fatty acid synthesis, and β-oxidation were reduced by ~50–80% in the white adipose tissue of Mac-PPARγ KO mice, indicating a global suppression of adipocyte function. Direct co-culture of PPARγ-deficient macrophages with adipocytes led to a marked reduction of insulin-stimulated glucose

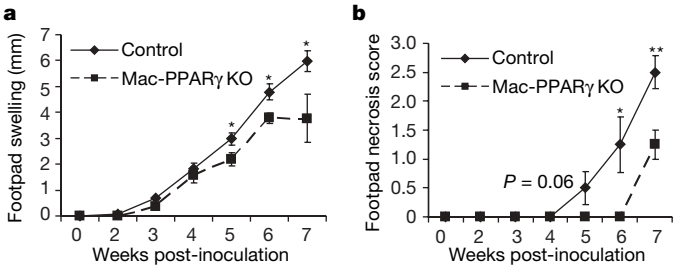

Figure 2 | Mac-PPARγ KO mice are less susceptible to infection by *Leishmania major*. **a**, Footpad swelling in control and Mac-PPARγ KO mice after infection with *L. major* ($n = 5$ per genotype). **b**, Decreased necrosis in footpads of Mac-PPARγ KO mice. Data presented as mean ± s.e.m. $^{*}P < 0.05$; $^{**}P < 0.01$.

uptake in adipocytes (Fig. 3d), suggesting a causal relationship between PPARγ-deficient adipose tissue macrophages (ATMs) and dysregulation of adipocyte metabolism. Remarkably, this was confirmed by Q-PCR analysis of co-cultured adipocytes, which showed suppression of adipocyte gene expression by PPARγ-deficient macrophages (Supplementary Fig. 4e).

To determine whether macrophage infiltration or aberrant activation contributed to adiposity, we analysed macrophage-specific gene expression in the white adipose tissue of control and Mac-PPARγ KO mice. Despite being more obese, transcript levels of macrophage-specific markers, *Emr1* and *CD68*, were reduced by ~70% in the white adipose tissue of Mac-PPARγ KO mice (Fig. 3e). Consistent with the Q-PCR data, histological analysis showed marked reduction in the macrophage content of the white adipose tissue of Mac-PPARγ KO mice (Fig. 3f, g). Importantly, expression of genes preferentially expressed in alternatively activated macrophages[10], such as *ArgI*, *Mrc1*, and *Clec7a*, was also decreased by ~70–80% in the white adipose tissue of Mac-PPARγ KO mice (Fig. 3e), suggesting that macrophage-specific deletion of PPARγ leads to specific reduction in alternatively activated macrophages. The absence of alternatively activated ATMs increased local inflammation in white adipose tissue, as shown by higher expression of *IL-6* and *Nos2* (Fig. 3e). Lastly, although ATM content is much lower in lean mice[3,9], Q-PCR analysis of white adipose tissue revealed that chow-fed (a low-fat diet) Mac-PPARγ KO mice expressed much lower levels of genes associated with the alternative state (Supplementary Fig. S5a).

While the Th2 cytokines IL-4 and IL-13 are required for maturation of alternatively activated macrophages during parasitic infections[10,14], the importance of this signalling pathway in ATM biology has not been formally tested. To determine whether IL-4/IL-13 signalling is required for acquisition of the alternative phenotype by ATMs, we analysed the molecular signature of ATMs in mice defective in IL-4/IL-13 signalling, in particular, the STAT6 null and Mac-IL-4Rα KO mice[14,20]. Consistent with a critical role for Th2 cytokines in alternative activation, the molecular signature of alternatively activated ATMs was dramatically reduced in lean STAT6 null and Mac-IL-4Rα KO mice (Supplementary Fig. 5b, c). Moreover, the expression profile of ATMs in obese STAT6 null mice was identical to

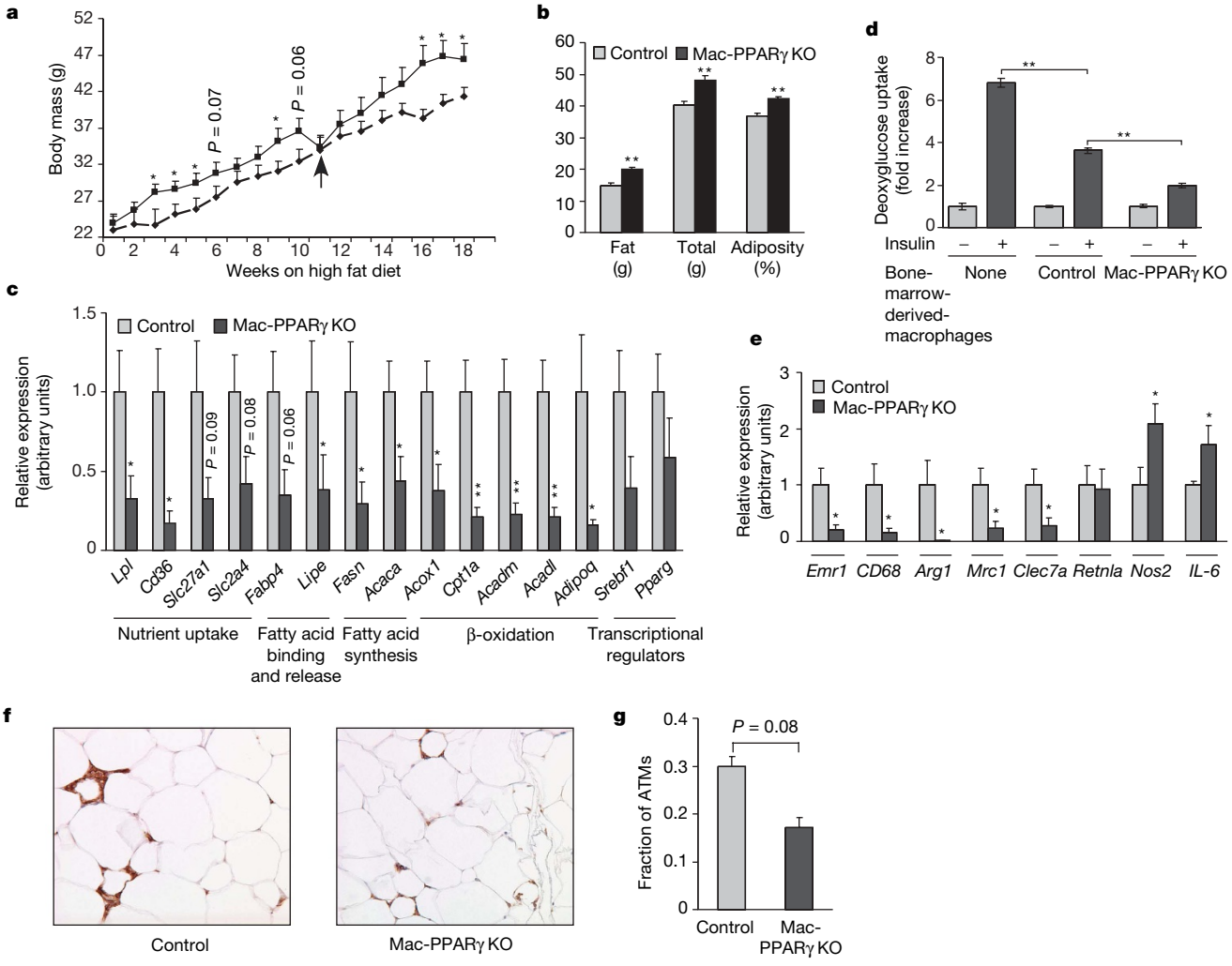

Figure 3 | Alterations in adipose tissue mass and function in Mac-PPARγ KO mice. **a**, Weight gain of control and Mac-PPARγ KO mice on a high fat diet. Arrow indicates mice fasted for glucose and insulin tolerance tests. **b**, Body composition as determined by dual-energy X-ray absorptiometry ($n = 5$ per genotype). **c**, Q-PCR analyses of gonadal adipose tissue gene expression. Relative transcript levels of genes involved in adipocyte differentiation and function. *Lpl*, lipoprotein lipase; *Cd36*, fatty acid translocase; *Slc27a1*, fatty acid transporter 1; *Slc2a4*, glucose transporter 4; *Fabp4*, fatty acid binding protein 4; *Lipe*, hormone sensitive lipase; *Fasn*, fatty acid synthase; *Acaca*, acetyl-Coenzyme A carboxylase a; *Acox1*, acyl-Coenzyme A oxidase 1; *Cpt1a*, carnitine palmitoyltransferase 1a; *Acadm* and *Acadl*, medium- and long-chain acyl-CoA dehydrogenase; *Adipoq*, adiponectin; *Srebf1*, sterol regulatory element binding factor 1c; *Pparg*, peroxisome proliferator activated receptor γ. **d**, Co-culture of macrophages with adipocytes decreases insulin-stimulated glucose uptake. **e**, Q-PCR analyses of macrophage gene expression in white adipose tissue from control and Mac-PPARγ KO mice. *Emr1*, F4/80; *Cd68*, macrosialin; *Arg1*, arginase I; *Mrc1*, mannose receptor; *Clec7a*, dectin-1; *Retnla*, resistin-like α; *Nos2*, inducible nitric oxide synthase; *IL-6*, interleukin-6. **f**, **g**, Macrophage content of white adipose tissue as assessed by F4/80 staining (**f**). Fraction of ATMs is equal to F4/80-stained cells/total cells counted in the fields (**g**). Data was statistically analysed using the paired Student's *t*-test (**g**). Data presented as mean ± s.e.m. $^*P < 0.05$; $^{**}P < 0.01$.

the profile observed in obese Mac-PPARγ KO mice (compare Fig. 3e and Supplementary Fig. 5d). The molecular signatures of ATMs in three distinct genetic models (Mac-PPARγ KO, STAT6 null and Mac-IL-4Rα KO) were similar, so our data show that an intact IL-4/IL-13/STAT6/PPARγ axis is required for maturation of alternatively activated ATMs. Furthermore, to investigate whether stimulation of ATMs by IL-4 is sufficient to polarize them towards the alternative state, obese control and Mac-PPARγ KO mice were injected with recombinant IL-4, and ATM gene expression was monitored by Q-PCR. Supplementary Fig. 5e shows that IL-4 induced the expression of alternatively activated markers (*Arg1*, *Chi3l3*, *Mrc1* and *Jag1*) in a PPARγ-dependent manner.

To explore the role of alternatively activated macrophages in obesity-induced insulin resistance, we performed glucose and insulin tolerance tests in control and Mac-PPARγ KO mice. Oral glucose tolerance tests revealed that Mac-PPARγ KO mice were significantly more glucose intolerant after an 18-week high fat diet challenge (Fig. 4a). As would be expected with a decrease in insulin sensitivity, Mac-PPARγ KO mice were more resistant to the glucose lowering effects of exogenous insulin (Fig. 4b). Moreover, after a 4-h fast, paired blood glucose and serum insulin levels were much higher in Mac-PPARγ KO mice, with blood glucose levels at $170 \pm 9.2\,mg\,dl^{-1}$ versus $125 \pm 2.3\,mg\,dl^{-1}$ ($P < 0.0007$) and serum insulin levels at ($3.00 \pm 0.77\,ng\,ml^{-1}$ versus $0.24 \pm 0.02\,ng\,ml^{-1}$ ($P < 0.002$), (Fig. 4c). The calculated homeostasis model assessment (HOMA) measure of insulin resistance was significantly higher in Mac-PPARγ KO mice (Fig. 4d). To investigate the potential sites of insulin resistance, control and Mac-PPARγ KO mice were injected with saline or insulin ($5\,mU\,g^{-1}$) through their inferior vena cava, and liver and skeletal muscle were quickly harvested for biochemical analysis. Strikingly, insulin-stimulated phosphorylation of AKT was markedly decreased in liver and skeletal muscle of Mac-PPARγ KO mice (Fig. 4e, f), findings consistent with the presence of insulin resistance in these tissues.

Mitochondrial dysfunction in muscle is associated with the onset of insulin resistance and type 2 diabetes[21–24], prompting us to examine mitochondrial gene expression in the skeletal muscles of obese mice. Q-PCR analyses showed that mRNAs encoding key enzymes in fatty acid oxidation (*Cpt1b*, *Acox1*) and oxidative phosphorylation (*Ndufs1*, *Sdh*, *Atp5j* and *Atp5b*) were reduced by 30–70% in the quadriceps muscles of Mac-PPARγ KO mice (Fig. 4g). Moreover, expression level of transcription factors and coactivator proteins controlling mitochondrial biogenesis[25,26], including *Tfam*,

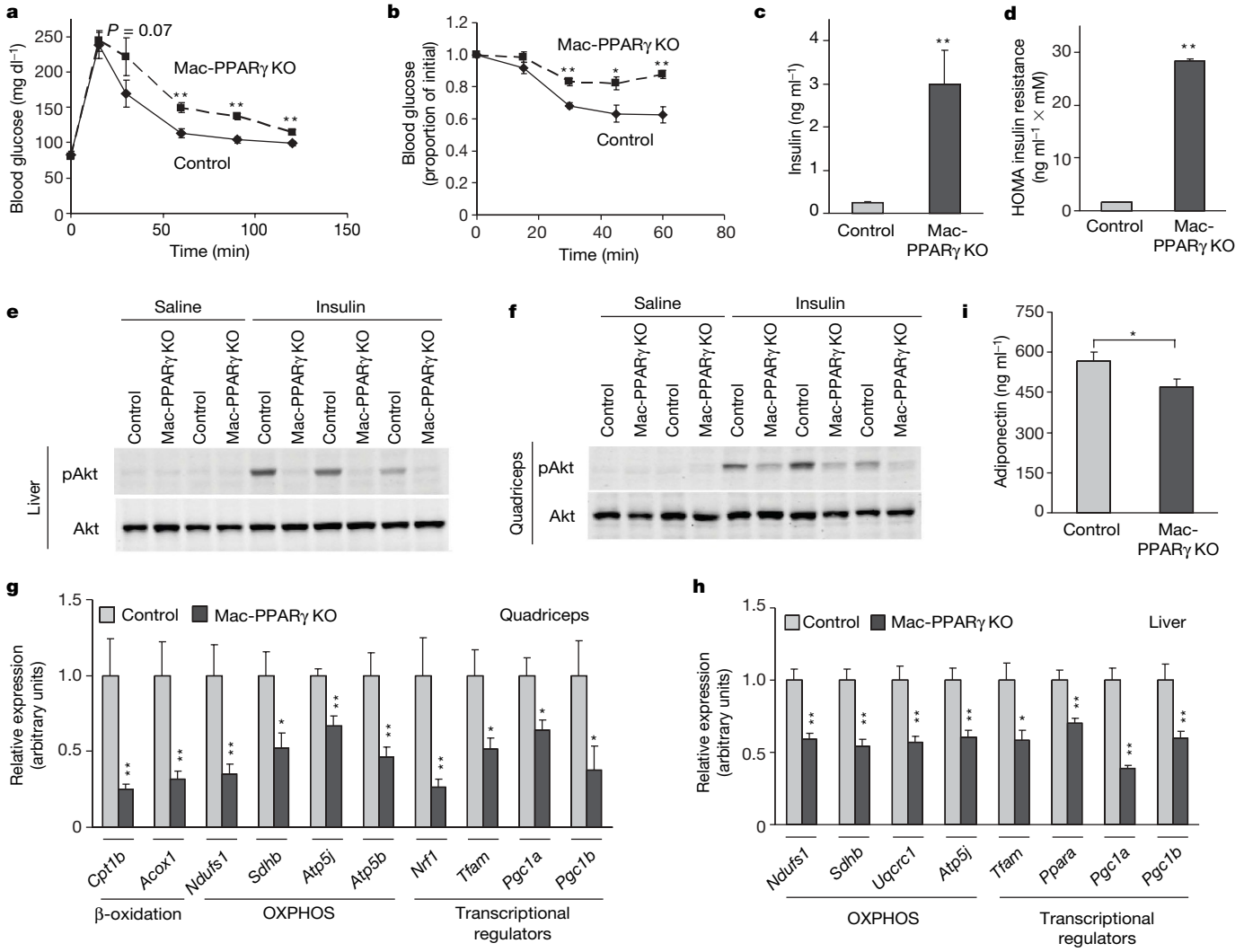

Figure 4 | Impaired glucose homeostasis in male Mac-PPARγ KO mice fed a high fat diet. **a**, Oral glucose tolerance tests ($1\,g\,kg^{-1}$) in male mice after 19 weeks of feeding the high fat diet ($n = 5$ per genotype). **b**, Insulin tolerance test. Obese mice were fasted for 4 h before intraperitoneal injection of insulin ($0.65\,U\,kg^{-1}$). **c**, Fasting serum insulin levels in control and Mac-PPARγ KO mice after a 4 h fast. **d**, The HOMA insulin resistance index of insulin sensitivity: insulin ($ng\,ml^{-1}$) × glucose (mM). **e**, **f**, Decreased insulin signalling in obese Mac-PPARγ KO mice. Cellular lysates were immunoblotted for the total amount of the oncoprotein Akt and for serine phosphorylated (S473) Akt in liver (**e**) and quadriceps (**f**). **g**, **h**, Relative transcript levels of various genes involved in β-oxidation and oxidative phosphorylation, and of transcriptional regulators controlling these pathways in quadriceps (**g**) and liver (**h**). **i**, Circulating levels of adiponectin in control and Mac-PPARγ KO mice. Data presented as mean ± s.e.m. $^*P < 0.05$; $^{**}P < 0.01$.

Nrf-1, *Pgc-1α* and *Pgc-1β*, was also reduced by 35–75% in the quadriceps of Mac-PPARγ KO mice (Fig. 4g). Similarly, expression of genes in the electron transport chain and their transcriptional regulators was reduced by 30–60% in the livers of Mac-PPARγ KO mice (Fig. 4h). Nonetheless, these livers did not display any overt signs of steatosis (Supplementary Fig. 6c, d), potentially reflecting their intact capacity to undergo β-oxidation (Supplementary Fig. 6e).

These findings suggest that direct or indirect effects of alternatively activated macrophages are important in maintaining oxidative capacity in skeletal muscle and liver. Because we did not observe significant differences in macrophage content or activation in liver and skeletal muscle of control and Mac-PPARγ KO mice (Supplementary Fig. 6a, b and data not shown), we focused on factors secreted by adipocytes that modulate oxidative metabolism in peripheral tissues[19,27]. Notably, recent studies have shown that adiponectin, a hormone specifically secreted by adipocytes, can induce PGC-1α and mitochondrial biogenesis in skeletal muscle[28]. Consistent with the global reduction in adipocyte function (Fig. 3c) and skeletal muscle oxidative capacity (Fig. 4g), the circulating level of adiponectin was reduced by ~18% in Mac-PPARγ KO mice (Fig. 4i). In contrast, serum levels of resistin, total cholesterol and triglycerides were similar in both strains of mice (Supplementary Table 1).

In summary, the requirement for PPARγ in expression of the alternatively activated phenotype, the absence of alternatively activated ATMs in Mac-PPARγ KO mice, and the observation that Mac-PPARγ KO mice are more susceptible to obesity and insulin resistance suggest that this program of macrophage activation protects against the metabolic consequences of obesity. In this setting of excess caloric intake, homeostatic functions performed by alternatively activated ATMs might allow animals to store and oxidize incoming lipids more efficiently, thereby maintaining insulin sensitivity and glucose tolerance. However, our findings raise additional issues that will require further investigation. First, to validate whether alternatively activated macrophages can be therapeutically exploited to treat type 2 diabetes, genetic and pharmacologic approaches that activate or inhibit IL-4 signalling in macrophages need to be tested. Second, although the presence of alternatively activated ATMs attenuates inflammation, we cannot exclude the possibility that remodelling activities of these cells might also lead to improvement in adipose tissue function. Lastly, in addition to their paracrine effects, it is plausible that peptides or lipids secreted by alternatively activated ATMs act in an endocrine fashion to modulate peripheral insulin sensitivity.

METHODS SUMMARY

For the generation of Mac-PPARγ KO mice, we backcrossed the (floxed) PPARγ$^{fl/+}$ mice, generated by the Gonzalez laboratory[29], for ten generations onto the Th2-permissive Balb/c background. To generate mice in which the PPARγ genes were disrupted in macrophages, PPARγ$^{fl/fl}$ Balb/c mice were mated with LysM^{Cre} mice, also on the Balb/c background[14]. Cohorts of PPARγ$^{fl/fl}$ (control) and PPARγ$^{fl/fl}$; LysM^{Cre} (Mac-PPARγ KO) mice were produced by intercrossing PPARγ$^{fl/fl}$ and PPARγ$^{fl/fl}$;LysM^{Cre} animals. Mice were genotyped for the presence of floxed and deleted alleles as described previously[29], and littermates were used to assemble the cohorts used in these studies.

Full Methods and any associated references are available in the online version of the paper at www.nature.com/nature.

Received 19 March; accepted 1 May 2007.
Published online 21 May 2007.

1. Shoelson, S. E., Lee, J. & Goldfine, A. B. Inflammation and insulin resistance. *J. Clin. Invest.* **116,** 1793–1801 (2006).
2. Hotamisligil, G. S. Inflammation and metabolic disorders. *Nature* **444,** 860–867 (2006).
3. Weisberg, S. P. *et al.* Obesity is associated with macrophage accumulation in adipose tissue. *J. Clin. Invest.* **112,** 1796–1808 (2003).
4. Xu, H. *et al.* Chronic inflammation in fat plays a crucial role in the development of obesity-related insulin resistance. *J. Clin. Invest.* **112,** 1821–1830 (2003).
5. Kanda, H. *et al.* MCP-1 contributes to macrophage infiltration into adipose tissue, insulin resistance, and hepatic steatosis in obesity. *J. Clin. Invest.* **116,** 1494–1505 (2006).
6. Kamei, N. *et al.* Overexpression of monocyte chemoattractant protein-1 in adipose tissues causes macrophage recruitment and insulin resistance. *J. Biol. Chem.* **281,** 26602–26614 (2006).
7. Weisberg, S. P. *et al.* CCR2 modulates inflammatory and metabolic effects of high-fat feeding. *J. Clin. Invest.* **116,** 115–124 (2005).
8. Gordon, S. & Taylor, P. R. Monocyte and macrophage heterogeneity. *Nature Rev. Immunol.* **5,** 953–964 (2005).
9. Lumeng, C. N., Bodzin, J. L. & Saltiel, A. R. Obesity induces a phenotypic switch in adipose tissue macrophage polarization. *J. Clin. Invest.* **117,** 175–184 (2007).
10. Gordon, S. Alternative activation of macrophages. *Nature Rev. Immunol.* **3,** 23–35 (2003).
11. Lehrke, M. & Lazar, M. A. The many faces of PPARγ. *Cell* **123,** 993–999 (2005).
12. Huang, J. T. *et al.* Interleukin-4-dependent production of PPAR-gamma ligands in macrophages by 12/15-lipoxygenase. *Nature* **400,** 378–382 (1999).
13. Vats, D. *et al.* Oxidative metabolism and PGC-1beta attenuate macrophage-mediated inflammation. *Cell Metab.* **4,** 13–24 (2006).
14. Herbert, D. R. *et al.* Alternative macrophage activation is essential for survival during schistosomiasis and downmodulates T helper 1 responses and immunopathology. *Immunity* **20,** 623–635 (2004).
15. Pauleau, A. L. *et al.* Enhancer-mediated control of macrophage-specific arginase I expression. *J. Immunol.* **172,** 7565–7573 (2004).
16. Evans, R. M., Barish, G. D. & Wang, Y.-X. PPARs and the complex journey to obesity. *Nature Med.* **10,** 355–361 (2004).
17. Alexander, J., Satoskar, A. R. & Russell, D. G. Leishmania species: models of intracellular parasitism. *J. Cell Sci.* **112,** 2993–3002 (1999).
18. Holscher, C., Arendse, B., Schwegmann, A., Myburgh, E. & Brombacher, F. Impairment of alternative macrophage activation delays cutaneous leishmaniasis in nonhealing BALB/c mice. *J. Immunol.* **176,** 1115–1121 (2006).
19. Rosen, E. D. & Spiegelman, B. M. Adipocytes as regulators of energy balance and glucose homeostasis. *Nature* **444,** 847–853 (2006).
20. Rutschman, R. *et al.* Cutting edge: Stat6-dependent substrate depletion regulates nitric oxide production. *J. Immunol.* **166,** 2173–2177 (2001).
21. Mootha, V. K. *et al.* PGC-1α-responsive genes involved in oxidative phosphorylation are coordinately downregulated in human diabetes. *Nature Genet.* **34,** 267–273 (2003).
22. Patti, M. E. *et al.* Coordinated reduction of genes of oxidative metabolism in humans with insulin resistance and diabetes: Potential role of PGC1 and NRF1. *Proc. Natl Acad. Sci. USA* **100,** 8466–8471 (2003).
23. Petersen, K. F. *et al.* Mitochondrial dysfunction in the elderly: possible role in insulin resistance. *Science* **300,** 1140–1142 (2003).
24. Vianna, C. R. *et al.* Hypomorphic mutation of PGC-1β causes mitochondrial dysfunction and liver insulin resistance. *Cell Metab.* **4,** 453–464 (2006).
25. Kelly, D. P. & Scarpulla, R. C. Transcriptional regulatory circuits controlling mitochondrial biogenesis and function. *Genes Dev.* **18,** 357–368 (2004).
26. Lin, J., Handschin, C. & Spiegelman, B. M. Metabolic control through the PGC-1 family of transcription coactivators. *Cell Metab.* **1,** 361–370 (2005).
27. Lazar, M. A. How obesity causes diabetes: not a tall tale. *Science* **307,** 373–375 (2005).
28. Civitarese, A. E. *et al.* Role of adiponectin in human skeletal muscle bioenergetics. *Cell Metab.* **4,** 75–87 (2006).
29. Akiyama, T. E. *et al.* Conditional disruption of the peroxisome proliferator-activated receptor gamma gene in mice results in lowered expression of ABCA1, ABCG1, and apoE in macrophages and reduced cholesterol efflux. *Mol. Cell. Biol.* **22,** 2607–2619 (2002).
30. Lumeng, C. N., Deyoung, S. M. & Saltiel, A. R. Macrophages block insulin action in adipocytes by altering expression of signaling and glucose transport proteins. *Am. J. Physiol. Endocrinol. Metab.* **292,** E166–E174 (2007).

Supplementary Information is linked to the online version of the paper at www.nature.com/nature.

Acknowledgements We thank members of the Chawla laboratory for comments, and A. Loh and C. H. Lee for critiquing the manuscript. We also thank P. Murray, J. McKerrow and O. McGuinness for providing key reagents and technical guidance. This work was supported by grants made available to A.C. from the NIH, the Astellas Foundation, Takeda Pharmaceuticals North America, the Rockefeller Brothers Fund and by Goldman Philanthropic Partnerships; and to A.W.F. from the NIH and Columbia DERC. A.C. is a Charles E. Culpeper Medical Scholar. Support was provided by Stanford MSTP (to J.I.O. and A.R.E.), the AHA (to J.I.O.), a HHMI Gilliam fellowship (to A.R.E.), the NRSA (to R.R.R.-G.), and an NIH Training Grant (to L.M.). All animal care was in accordance with Stanford University's A-PLAC committee guidelines.

Author Contributions J.I.O and R.R.R.-G were involved in project planning, experimental work and data analysis; M.H.G, C.R.M, V.S, L.M., D.V. and A.R.E. performed experimental work; F.B. was involved in project planning; and A.W.F. and A.C. were involved in project planning, data analysis and manuscript preparation.

Author Information Reprints and permissions information is available at www.nature.com/reprints. The authors declare no competing financial interests. Correspondence and requests for materials should be addressed to A.C. (achawla@stanford.edu).

METHODS

Functional analysis for alternative macrophage activation. Bone-marrow-derived macrophages from control, Mac-PPARγ KO and PPARδ$^{-/-}$ (on the 129Sv background) mice were cultured as described in previously[13]. To promote alternative macrophage activation, bone-marrow-derived macrophages were stimulated with IL-4 (10 ng ml^{-1}) for 24–96 h. Arginase I activity was monitored via a colorimetric assay that detects the production of urea[15]. Fatty acid oxidation rates in macrophages were quantified using the sodium hydroxide trap in a modified tissue culture flask[13]. Cellular mitochondrial content was quantified using MitoTracker dyes (Molecular Probes), according to the manufacturer's instructions. All assays were performed in duplicate or triplicate and repeated at least three independent times, and total cell number or protein content was used for normalization of the data.

Gel mobility shift assays and transient transfections. *In vitro* translated proteins (TNT kit, Promega) and ^{32}P end-labelled oligonucleotides were used to carry out the gel mobility shift assays. Competition assays were performed with excess unlabelled oligonucleotides. The acyl-CoA oxidase PPAR response element served as a positive control for these studies. The sequence of the arginase I PPAR response element is (two half sites separated by a base pair): AAGTCA G AGAGCA. Transient transfection experiments were performed in RAW 264.7 cells. Briefly, cells were electroporated via the GenePulser II (BioRad) at 300 V, 1,000 μF, and allowed to recover overnight. Luciferase assays were performed 16–20 h after stimulation with IL-4 (10 ng ml^{-1}) or rosiglitazone (1 μM) with the Dual-Luciferase reporter assay system (Promega). The phRL-null plasmid (Promega) was used as an internal control to monitor transfection efficiency. All transfections were done in triplicate and repeated at least three times.

Immunoblots, ELISAs and immunohistochemistry. Total cellular proteins were immunoblotted for cytochrome C (1:1,000, BD Pharmingen), VDAC1 (1:2000, Molecular Probes), and β-actin (1:5,000, Sigma). Infrared dye (IR Dye 800) conjugated secondary antibodies (1:30,000, Rockland) were used for protein detection. For ELISAs, macrophages pre-treated with IL-4 (10 ng ml^{-1}) for 24 h were subsequently stimulated with lipopolysaccharide (5 ng ml^{-1}) for 6 h (TNFα) or 24 h (IL-6). Cytokine secretion was quantified by ELISA, according to the manufacturer's protocols (BD Pharmingen). All assays were done in triplicate and repeated at least three independent times. Macrophages in the gonadal fat pads were visualized by F4/80 immunostaining and quantified as described previously[7].

Gene expression analysis. Trizol reagent (Invitrogen) was used to prepare total RNA from macrophages or tissues. Total RNA (2 μg) was treated with DNase (1 U ml^{-1}) and reverse transcribed using a first-strand complementary DNA synthesis kit (Marligen). Q-PCR assays were carried out in triplicate on the DNA Engine Opticon 2 real-time PCR detection system. Relative expression levels for mRNAs were calculated using the comparative C_T method normalized to the L32 RNA.

***Leishmania* infection.** *Leishmania major* (strain WHOM/IR/-/173) promastigotes were cultured at 27 °C in M199 containing 15% fetal bovine serum, 100 U ml^{-1} penicillin, 2 mM glutamine, 100 μM adenine, 5 μg ml^{-1} haemin, and 40 mM HEPES. Stationary phase metacyclic promastigotes (2×10^6) were injected into the left hind footpad[18]. Footpad thickness was measured weekly using a caliper (Mitutoyo), and reported as the difference in thickness between the infected and uninfected footpads. Footpad necrosis was graded using the following scale: 0, no visible abscesses; 1, one or more visible subcutaneous abscesses; 2, point surface necrosis; 3, surface necrosis over <50% of foot pad; 4, surface necrosis over >50% of foot pad; and 5, death of the foot.

Metabolic studies. Mice were fed a high fat diet (Bio-Serv F3282) to promote obesity. Oral glucose tolerance tests (1 g kg^{-1}) were performed after an overnight fast. For the insulin tolerance test, mice were fasted for 4 h before injection of human regular insulin (0.65 U kg^{-1}). Tail blood glucose levels were monitored at 0, 15, 30, 60 and 120 min time points with the Bayer Elite glucometer. For biochemical analysis of insulin signalling, obese mice of both genotypes were injected with insulin (5 mU g^{-1}) through their inferior vena cavas after a 4 h fast. Liver and quadriceps were isolated 2 and 5 min, respectively, after insulin injection. Homogenized proteins were immunoblotted for total Akt and phospho-Akt (S473, Cell Signaling). Serum levels of adipokines (leptin, adiponectin and resistin), cytokines (TNFα, IL-6 and IL-1β), lipids (total cholesterol and triglycerides), and insulin in fasted mice was quantified using commercially available kits.

Macrophage/adipocyte co-culture. Macrophage/adipocyte direct co-culture experiments were performed as described previously[30]. Briefly, 100,000 bone-marrow-derived macrophages (day 10) were co-incubated with differentiated 3T3-L1 adipocytes (day 8) for 48 h. Cultures were stimulated with insulin (100 nM) for 30 min, and glucose uptake was monitored using 0.2 mM 2-[^{3}H] deoxyglucose (1 μCi ml^{-1}) over 5 min. Incorporated radioactivity was normalized for protein content, and expressed as fold increase over untreated samples.

Statistical analysis. Data are presented as mean ± s.e.m., and Student's *t*-test (two-tailed distribution, two-sample unequal variance) was used to calculate the *P* value. Statistical significance is displayed as $P < 0.05$ (one asterisk) or $P < 0.01$ (two asterisks).